JACS
JOURNAL OF THE AMERICAN CHEMICAL SOCIETY
pubs.acs.org/JACS
Article

Reduction of Dinitrogen via 2,3′-Bipyridine-Mediated Tetraboration

Longfei Li,* Zeyu Wu, Huajie Zhu,* Gregory H. Robinson, Yaoming Xie, and Henry F. Schaefer*

Cite This: J. Am. Chem. Soc. 2020, 142, 6244−6250
Read Online
ACCESS | Metrics & More | Article Recommendations | Supporting Information

ABSTRACT: A new molecular system for nitrogen reduction, involving a 2,3′-bipyridine-anchored, end-on-bridging dinitrogen complex of the $Me_2B{-}BMe_2$ intermediate (**4**), has been explored by theoretical methods. The 2,3′-bipyridine-mediated cleavage of the $B_{sp3}{-}B_{sp3}$ bond in **4** may lead to transient electron-rich sp^3-hybridized boron species and subsequent activation of the strong N≡N triple bond of the complexed N_2. Through a boryl transfer sequence, a catalytic cycle may be achieved for the reductive addition of diboranes to a dinitrogen molecule with an energy span of 23 kcal/mol. In addition, the reaction is exothermic by 80.5 kcal/mol, providing a substantive chemical driving force.

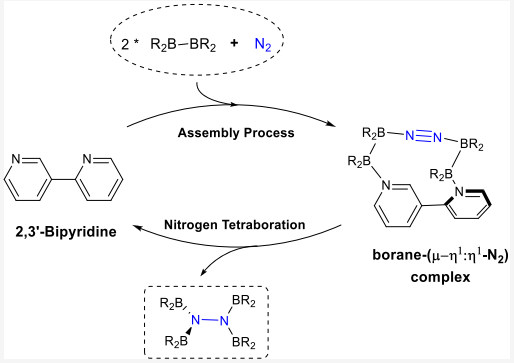

INTRODUCTION

Due to the nonpolarity and extremely high bond energy of the N≡N triple bond (ca. 225 kcal/mol),[1] molecular nitrogen (N_2) (making up appropriately 78% of air) is unusually stable. Nitrogen-fixation, reducing molecular nitrogen to ammonia, is achieved naturally by nitrogenases via multiple proton−electron transfers.[2−4] The industrial Haber−Bosch process, utilized for the conversion of N_2 and H_2 to NH_3, supports half of all global food production. However, this process is conducted under harsh reaction conditions (350−550 °C and 150−350 atm) and consumes about 2% of the annual worldwide energy production.[5,6] In the context of energy and climate change challenges, the development of energy-efficient and environmentally benign strategies for N_2 reduction reaction (NRR), such as electrocatalytic N_2 reduction, is highly desirable and being actively investigated.[7−9] However, to date, all electrochemical NRRs suffer from low yield rates (TON < 100) and poor selectivity, due to the competitive $2H^+/2e^-$ hydrogen evolution reaction.[10,11] In order to improve the efficiency of NRR, many other methods, including biological and biomimetic approaches,[12] heterogeneous thermocatalytic processes,[13] photocatalytic processes,[14−16] and plasma-mediated N_2 fixation[17] have been explored. Although considerable progress has been made, it is important for scientists to develop more efficient methods for NRR.[18,19]

Transition metal-based N_2 fixation and activation involves not only σ-donation of the lone pair of electrons of N_2 into empty d orbitals but also π-back-donation of filled d orbitals of the metal center into the unoccupied π^* orbital of N_2 (i.e., Dewar-Chatt-Duncanson bonding model) (Scheme 1a).[20,23] The π-back-donation weakens the N−N bond and thus plays a key role in N_2 activation. A series of Mo and Fe molecular catalysts for NRR, through the addition of $6H^+/6e^-$ into a weakened dinitrogen ligand, have been documented.[24−27] The Chatt-type (distal) and alternating pathways have been proposed for mechanistic outlines.[28−30] In contrast to electron-rich transition metals, high-oxidation-state uranium(V) is electron-poor (with only one 5f valence electron) and thus not a good candidate for N_2 binding. However, recently, Liddle and co-workers achieved a rare end-on uranium(V)-dinitrogen complex by utilizing both cooperative heterobimetallic uranium−lithium effects and electron-rich ancillary ligands that result in back-donation of the uranium(V) ion into π^* orbital of N_2.[31]

Due to their low cost and wide abundance, main group elements have been employed to mimic transition metals in small molecule activation and even potential catalytic applications.[32] Dinitrogen complexation with main group radicals has been probed by the electron paramagnetic resonance (EPR) technique.[33] Indeed, Braunschweig and co-workers[21] discovered that carbene-complexed dicoordinate borylene, as a transient electron-rich B(I) species, may mimic transition metals to reduce dinitrogen via p → π_{NN}^* backbonding interactions (Scheme 1b). Subsequent to the discovery of borylene-mediated N_2 reduction,[21] a series of boron-doped two-dimensional materials have been explored as metal-free electro- or photocatalysts for N_2 reduction by both experimental and theoretical methods.[34−41] Notably, a theoretical study proposed that the sp^3-hybridized boron

Received: January 13, 2020
Published: March 11, 2020

https://dx.doi.org/10.1021/jacs.0c00409
J. Am. Chem. Soc. 2020, 142, 6244−6250

Scheme 1. Schematic Representations of the End-on Bonding Modes in Transition Metal N_2 Complexes (a),[20] Dicoordinate Borylene N_2 Complexes (b),[21] and Single sp^3-Hybridized Boron Atom (Decorated on g-C_3N_4) N_2 Complexes (c)[22]

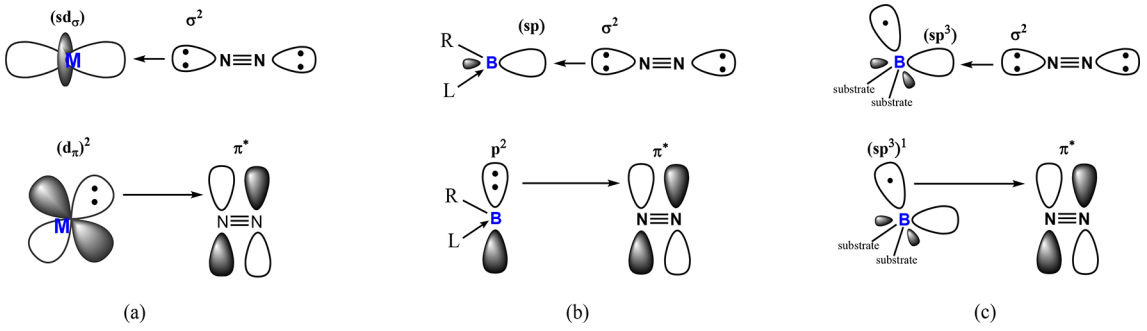

atom, decorated on the optically active graphitic-carbon nitride (B/g-C_3N_4), may enable solar-driven N_2 fixation.[22] In this case, one vacant and one occupied sp^3-hybridized orbital of the boron atom give rise to the bonding interactions with N_2 (Scheme 1c). While diboranes without π-donating function (such as H_2B-BH_2) may weakly coordinate N_2 to provide traditional Lewis adducts,[42−45] diborane(4)-based N_2 reduction reactions have yet to be reported. Inspired by recent silico reaction discoveries,[46,47] we demonstrate our theoretical study on 2,3′-bipyridine-mediated N_2 reduction by a diborane(4), namely, Me_2B-BMe_2.

COMPUTATIONAL METHODS

This research was carried out with the DFT ωB97X-D[48] method using the Gaussian 09 programs.[49] All the structures were optimized in benzene solvent (with a low dielectric constant; ε = 2.2706) using the SMD (Solution Model based on Density) solvation model. The 6-311++G** basis sets were used in the geometry optimization.[50,51] All transition states were confirmed to exhibit only one imaginary frequency via Hessian analyses. Intrinsic reaction coordinate (IRC) calculations were performed to confirm that all transition states connect the two related minima. The wave function stability was checked for all the stationary points, and the wave functions of all structures, including minima and transition states, are found to be stable. The present transformation involves a multicomponent change; thus, entropy overestimations must be taken into account.[52−54] In this study, translational movement was evaluated using the method presented by Whitesides and co-workers.[55] Natural bond orbital (NBO) analyses were performed using the NBO 6.0 program.[56] We have thoroughly examined the conformational space of each intermediate and transition state, and the lowest energy conformers are included in the discussion. The Cartesian coordinates of all optimized structures are presented in the Supporting Information.

RESULTS AND DISCUSSIONS

Pyrazines have been reported to undergo addition of B−B bonded boron reagents. After that, 4,4′-bipyridines-catalyzed diboration of sterically demanding pyrazines has been achieved.[55] These discoveries suggest that nitrogen-containing bases may not only conduct reductive addition by cleaving the boron−boron bond of diborons but also readily release the boryl groups to pyrazine subtrates.[57−59] Herein, we propose a novel strategy for NRR through an unusual N_2 activation mode (Figure 1). This strategy involves building an interconnected bis(Lewis base)-anchored, end-on-bridging dinitrogen complex of diboranes(4) (Figure 1c), which may subsequently undergo catalytic tetraboration of dinitrogen.

In the present study, 2,3′-bipyridine **1** was selected as the bis(Lewis base)-anchor ligand because its N···N distance is

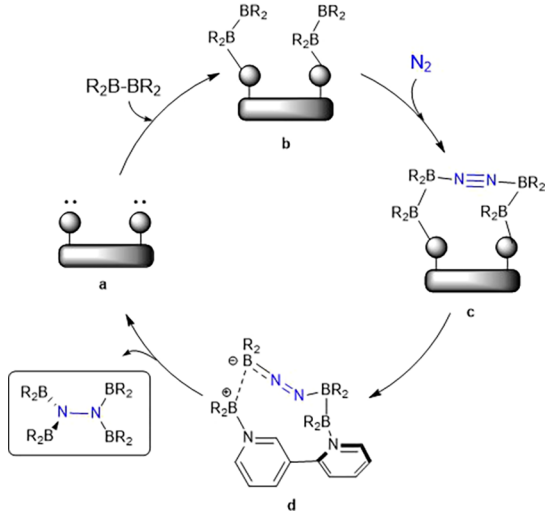

Figure 1. Proposed bis(Lewis-base)-catalyzed tetraboration reaction of N_2. Structure (a) stands for the bis(Lewis base) ancillary ligand.

suitable to intermediates such as structure **4**, while Me_2B-BMe_2 was chosen as a diborane model (Figure 2). With two anchor sites (i.e., nitrogen atoms), **1** can bind two Me_2B-BMe_2 molecules through classical donor−acceptor bonds to give **2**, which is predicted to be exothermic by 9.1 kcal/mol. Notably, the two terminal boron atoms in **2** are sp^2 hybridized and thus form a suitable borane pocket for the capture of one dinitrogen molecule. The dinitrogen molecule coordination proceeds in a stepwise manner. Consequently, intermediate **3** with an end-on N_2 ligand is generated first (Figure 2). Through the transition state **TS3−4**, the N_2 ligand in **3** binds to the other terminal B_{sp2} atom in an end-on fashion, providing the Lewis-base-anchored diborane-($\mu-\eta^1:\eta^1$-N_2) complex **4**. The energy span for the assembly of **4** is 22.6 (= 9.1 + 13.5) kcal/mol. This suggests that the intermediates **4** may exist under mild conditions. Although the classical energy (ΔE) of **TS3−4** is higher than **4** by 1.4 kcal/mol, the Gibbs free energy (ΔG) for **TS3−4** is 0.3 kcal/mol lower than that of **4**. The B1−B2 distance in **4** is 1.883 Å (Figure 3), which is significantly longer than that in free Me_2B-BMe_2 molecule (1.678 Å), suggesting that the synergetic coordination of 2,3′-bipyridine and N_2 would favor cleavage of the B−B bond of Me_2B-BMe_2. The B−B cleavage of Me_2B-BMe_2 across two nitrogen atoms of **1** was also investigated. The generated **9** (Figure S1 in Supporting Information) is less favored than **2**.

Our results for the $B_{sp3}-B_{sp3}$ bond cleavage in **4** are shown in Figure 4. Due to the lability of the $B_{sp3}-B_{sp3}$ bond in **4**, its

https://dx.doi.org/10.1021/jacs.0c00409
J. Am. Chem. Soc. 2020, 142, 6244−6250

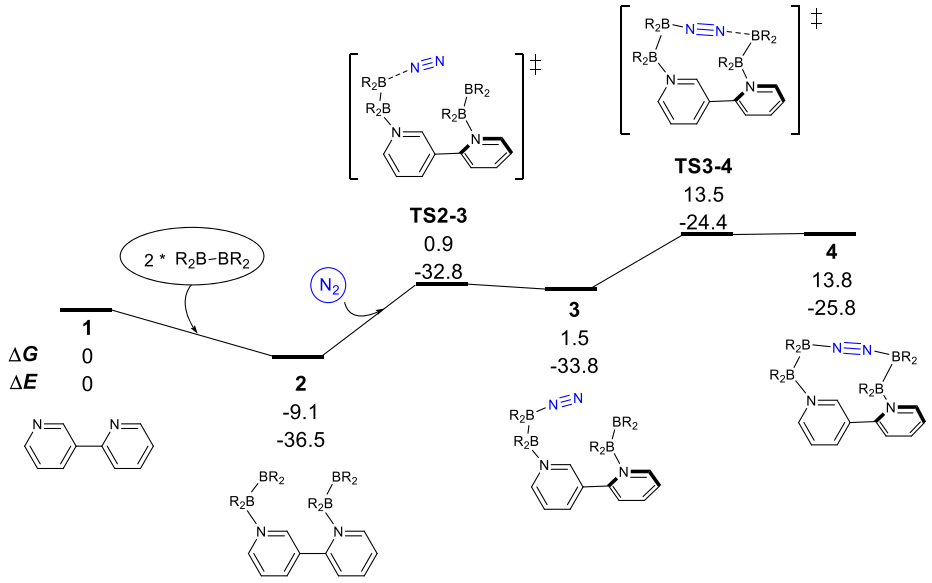

Figure 2. Profile of Gibbs free energies (upper, in kcal/mol at 298.15 K and 1 atm pressure) and classical energies (lower, in kcal/mol) for the assembly of **4** (R = Me). All structures were optimized in benzene.

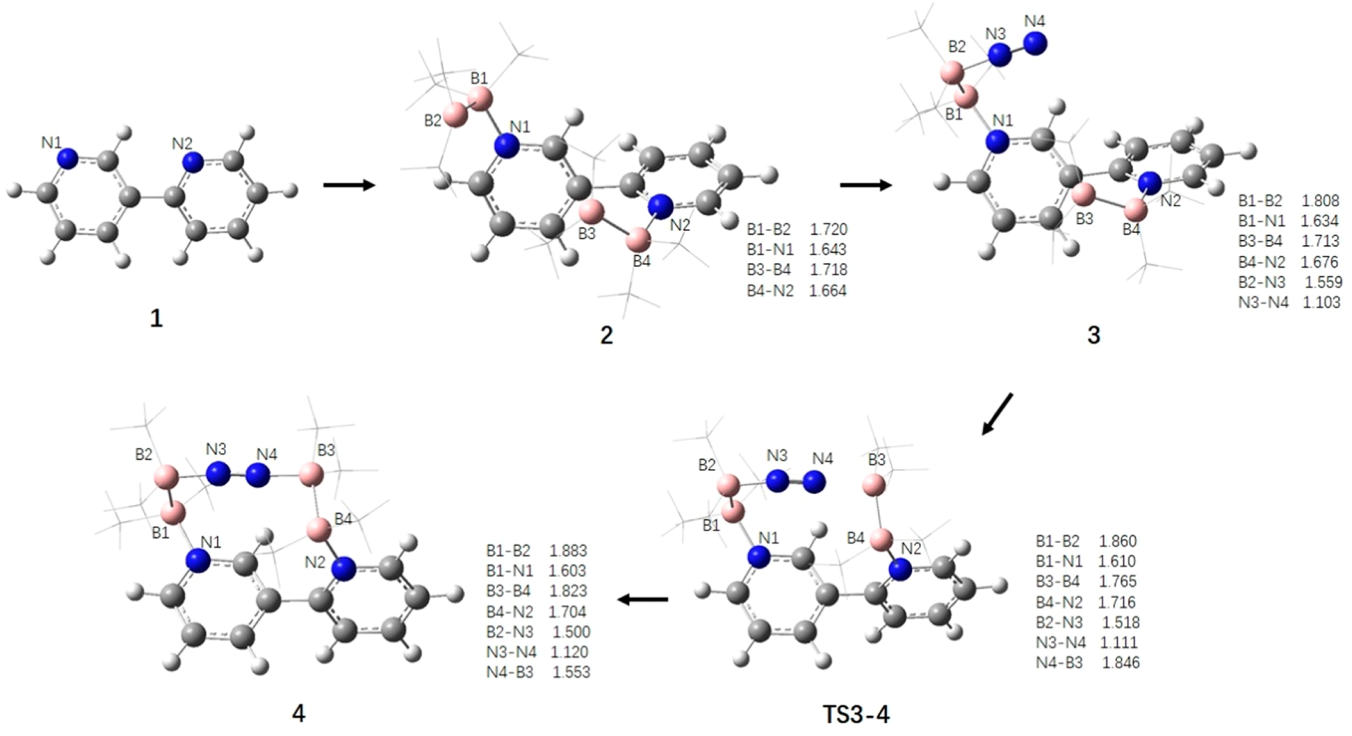

Figure 3. Structures involved in the assembly of **4**. The internuclear separations are given in Å. The methyl groups on the boron atoms are drawn in wireframe for simplicity. All structures were optimized in benzene.

cleavage should be facile with a low energy barrier of 0.4 kcal/mol. The IRC result indicates that **TS4−5** connects with another intermediate **5**, which lies 18.1 kcal/mol lower than **4**. Along with the cleavage of the B(1)−B(2) bond, the N(4) atom with a lone pair is bonded to the C(1) atom next to the N(1) atom of the pyridine ring with a single carbon−nitrogen bond length of 1.534 Å (Figure 5). The C−N bond formation in **5** is energetically favorable, because it avoids the high-energy XN=NX structure.[60] The natural atomic charges for B(1) (+1.02) and N(3) (−0.35) atoms are computed. The N−N bond distance of the complexed N_2 moiety is elongated by ca. 0.1 Å from **4** to **5**, whereas the B(2)−N(3) bond distance is correspondingly decreased from 1.500 Å (for **4**) to 1.382 Å (for **5**). Therefore, we can draw the conclusion that the cleavage of the B_{sp3}−B_{sp3} bond in **TS4−5** would lead to the activation of N≡N triple bonds, and this finding may be ascribed to the formation of transient sp^3-hybridized B^- atom that back-donates the electron density to the π^* orbital of N_2 (Figure 6).

The subsequent boryl transfer steps experienced by **5** finally result in the release of a reduced nitrogen product $(BMe_2)_2N$−$N(BMe_2)_2$ through a downhill energy pathway with low

https://dx.doi.org/10.1021/jacs.0c00409
J. Am. Chem. Soc. 2020, 142, 6244−6250

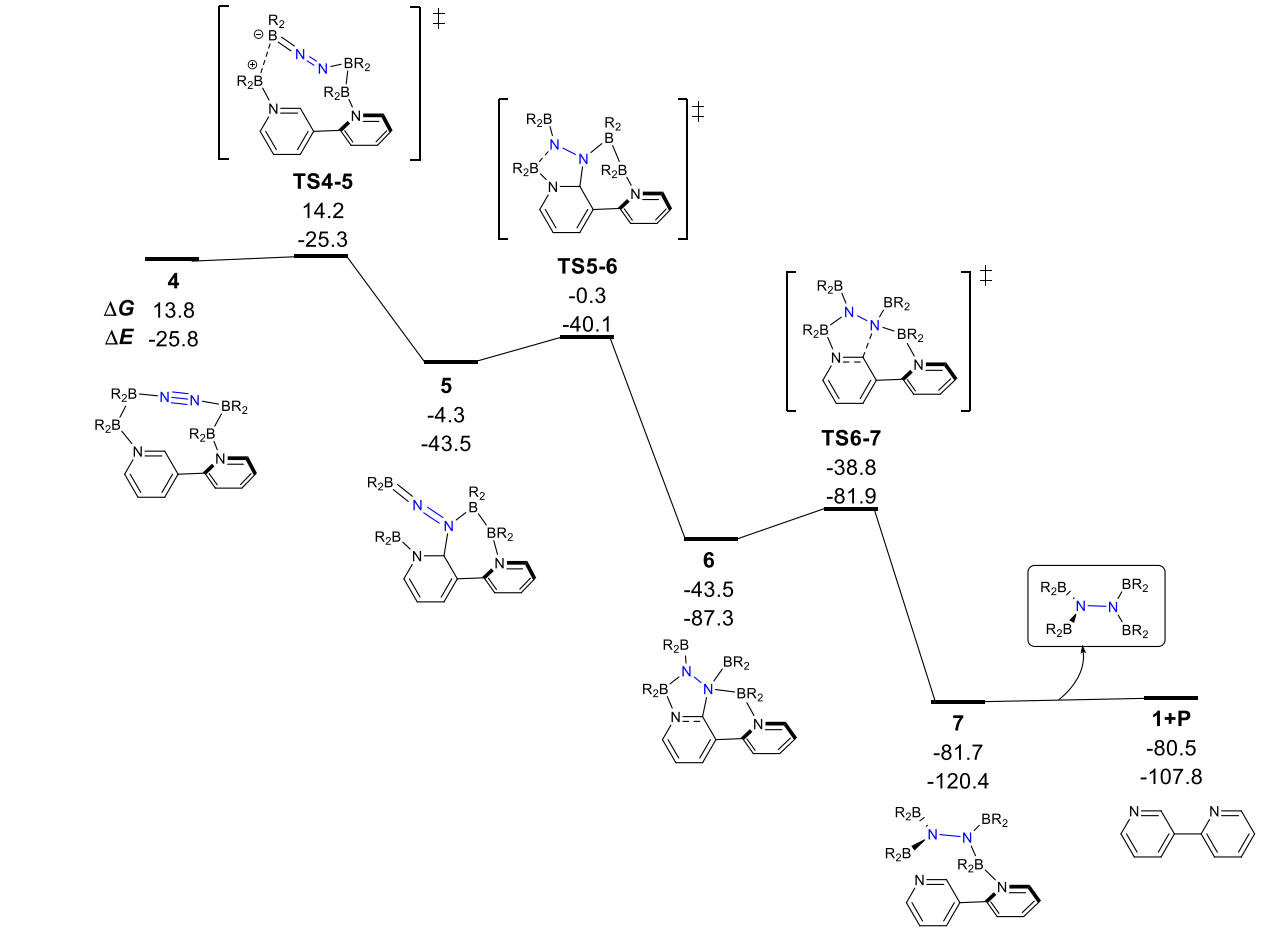

Figure 4. Profile of Gibbs free energies (upper, in kcal/mol at 298.15 K and 1 atm pressure) and classical energies (lower, in kcal/mol) for 2,3′-bipyridine-mediated reductive tetraboration of N_2 (R = Me). All structures were optimized in benzene.

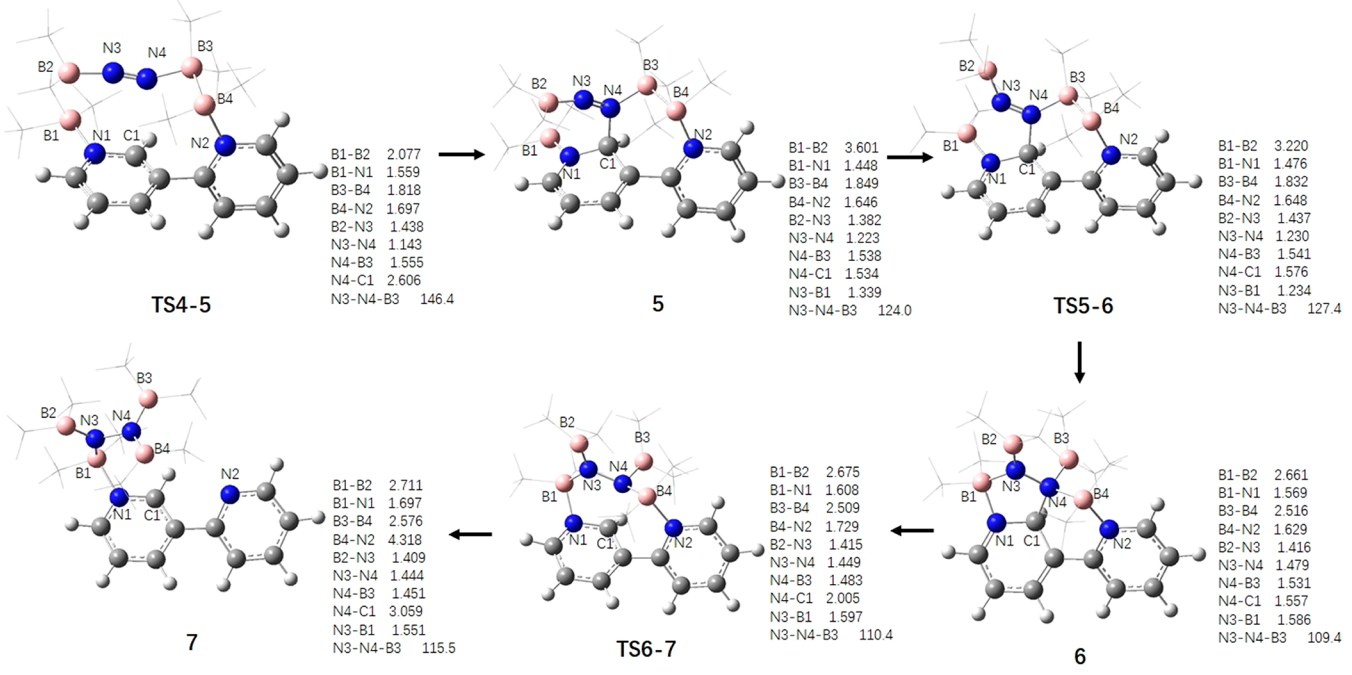

Figure 5. Structures accompanying 2,3′-bipyridine-mediated reductive tetraboration of N_2. The internuclear separations are given in Å. The methyl groups on the boron atoms are drawn in wireframe for simplicity. All structures were optimized in benzene.

https://dx.doi.org/10.1021/jacs.0c00409
J. Am. Chem. Soc. 2020, 142, 6244−6250

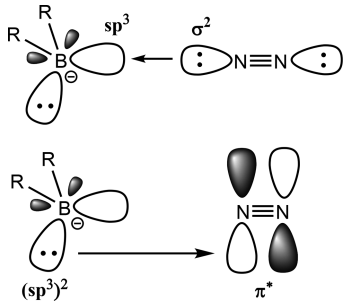

Figure 6. End-on bonding modes for N_2 with the sp^3-hybridized B^- atom in the transition state **TS4−5**.

barriers (Figure 4). The Lewis basic N(3) atom in **5** approaches the Lewis acidic B(1) atom via the transition state **TS5−6** (with an energy barrier of 4 kcal/mol), giving an intermediate **6**, which is favored in energy with respect to **5** by 39.2 kcal/mol. The transition state **TS6−7** involves both N(4)−C(1) and B(4)−N(2) bond cleavage, and leads to intermediate **7**, an adduct of bipyridine **1** with $(BMe_2)_2N-N(BMe_2)_2$. The cleavage of the C−N bond is energetically favored in this step because two strong B−N−B conjugation arrangements are obtained in the generated $(BMe_2)_2N-N(BMe_2)_2$ moiety of intermediate **7**. Thus, the step from **6** to **7** is exothermic by 38.2 kcal/mol. The final dissociation of $(BMe_2)_2N-N(BMe_2)_2$ is expected to regenerate the starting species **1**, thereby affording a complete catalytic cycle (Figure 1). The production of $(BMe_2)_2N-N(BMe_2)_2$ (as shown in Figure 4) experiences a substantial energy decrease of 80.5 kcal/mol, which provides the important chemical driving force for the catalytic reaction.

The effects of temperature, pressure, and solvent on the Gibbs free energies are included in this study, and these conditions do not change the free energy span significantly (Tables S3−S5 in SI). Table S3 shows that the free energy span is from 22 kcal/mol at 273 K to 27 kcal/mol at 373 K, with the low temperature slightly in favor of the reaction. When the pressures increased from 1 to 2 atm, the energy span changes by only 0.4 kcal/mol (Table S4 in SI), and the three different solvents (benzene, trichloromethane, and dichlorometnae) predict a very close energy span within 0.5 kcal/mol (Table S5 in SI).

CONCLUSIONS

While the bonding interaction between diborane(4) and N_2 is reportedly weak, the present study suggests that a 2,3′-bipyridine-anchored diborane pocket may be utilized in both capturing an N_2 molecule and in its activation. Our research study unveils an unprecedented N_2 activation mode: the boron−boron bond cleavage of the Me_2B-BMe_2 moiety in **4** leading to a transient sp^3-hybridized B^- atom and donating electron density to the π^* orbital of N_2. The complete catalytic cycle includes both an assembly process (giving **4**) and a boryl transfer sequence (yielding the $(BMe_2)_2N-N(BMe_2)_2$ product and regenerating the bipyridine **1**). The corresponding energy span of 23.3 kcal/mol (= 14.2 + 9.1) indicates that this conversion is kinetically feasible under mild conditions. In addition, this catalyzed reaction is thermodynamically favorable with a reaction free energy of −80 kcal/mol. We hope that the present study will provide strong motivation for further studies on NRR.

ASSOCIATED CONTENT

Supporting Information

The Supporting Information is available free of charge at https://pubs.acs.org/doi/10.1021/jacs.0c00409.

Optimized geometries and energies of all stationary points along the reaction pathways, the imaginary vibrational frequencies of transition states (PDF)

AUTHOR INFORMATION

Corresponding Authors

Longfei Li − *College of Pharmacy, Hebei University, Baoding 071002, Hebei, People's Republic of China*; Email: lilongfei@hbu.edu.cn

Huajie Zhu − *College of Pharmacy, Hebei University, Baoding 071002, Hebei, People's Republic of China*; Email: zhuhuajie@hotmail.com

Henry F. Schaefer − *Department of Chemistry and Center for Computational Quantum Chemistry, University of Georgia, Athens, Georgia 30602, United States*; orcid.org/0000-0003-0252-2083; Email: ccq@uga.edu

Authors

Zeyu Wu − *College of Pharmacy, Hebei University, Baoding 071002, Hebei, People's Republic of China*

Gregory H. Robinson − *Department of Chemistry and Center for Computational Quantum Chemistry, University of Georgia, Athens, Georgia 30602, United States*; orcid.org/0000-0002-2260-3019

Yaoming Xie − *Department of Chemistry and Center for Computational Quantum Chemistry, University of Georgia, Athens, Georgia 30602, United States*

Complete contact information is available at: https://pubs.acs.org/10.1021/jacs.0c00409

Notes

The authors declare no competing financial interest.

ACKNOWLEDGMENTS

This work was supported by the National Natural Science Foundation of China (No. 21903018, 21877025), the Natural Science Foundation of Hebei Province of China (No. B2019201128). The research at the University of Georgia was supported by National Science Foundation (HFS: CHE 1661604 and GHR: CHE-1855641). We thank the High Performance Computer Center of Hebei University for providing the computational resources.

REFERENCES

(1) Ren, X.; Zhao, J.; Wei, Q.; Ma, Y.; Guo, H.; Liu, Q.; Wang, Y.; Cui, G.; Asiri, A. M.; Li, B.; Tang, B.; Sun, X. High-Performance N_2-to-NH_3 Conversion Electrocatalyzed by Mo_2C Nanorod. *ACS Cent. Sci.* **2019**, *5*, 116−121.

(2) Hoffman, B. M.; Lukoyanov, D.; Yang, Z.-Y.; Dean, D. R.; Seefeldt, L. C. Mechanism of Nitrogen Fixation by Nitrogenase: The Next Stage. *Chem. Rev.* **2014**, *114*, 4041−4062.

(3) Cai, R.; Minteer, S. D. Nitrogenase Bioelectrocatalysis: From Understanding Electron-Transfer Mechanisms to Energy Applications. *ACS Energy Lett.* **2018**, *3*, 2736−2742.

(4) Milton, R. D.; Minteer, S. D. Nitrogenase Bioelectrochemistry for Synthesis Applications. *Acc. Chem. Res.* **2019**, *52*, 3351−3360.

(5) Li, J.; Li, H.; Zhan, G.; Zhang, L. Solar Water Splitting and Nitrogen Fixation with Layered Bismuth Oxyhalides. *Acc. Chem. Res.* **2017**, *50*, 112−121.

(6) van der Ham, C. J.; Koper, M. T.; Hetterscheid, D. G. Challenges in reduction of dinitrogen by proton and electron transfer. *Chem. Soc. Rev.* **2014**, *43*, 5183−5191.
(7) Choi, C.; Back, S.; Kim, N.-Y.; Lim, J.; Kim, Y.-H.; Jung, Y. Suppression of Hydrogen Evolution Reaction in Electrochemical N_2 Reduction Using Single-Atom Catalysts: A Computational Guideline. *ACS Catal.* **2018**, *8*, 7517−7525.
(8) Guo, W.; Zhang, K.; Liang, Z.; Zou, R.; Xu, Q. Electrochemical nitrogen fixation and utilization: theories, advanced catalyst materials and system design. *Chem. Soc. Rev.* **2019**, *48*, 5658−5716.
(9) Guo, X.; Du, H.; Qu, F.; Li, J. Recent progress in electrocatalytic nitrogen reduction. *J. Mater. Chem. A* **2019**, *7*, 3531−3543.
(10) Suryanto, B. H. R.; Kang, C. S. M.; Wang, D.; Xiao, C.; Zhou, F.; Azofra, L. M.; Cavallo, L.; Zhang, X.; MacFarlane, D. R. Rational Electrode-Electrolyte Design for Efficient Ammonia Electrosynthesis under Ambient Conditions. *ACS Energy Lett.* **2018**, *3*, 1219−1224.
(11) Iwamoto, M.; Akiyama, M.; Aihara, K.; Deguchi, T. Ammonia Synthesis on Wool-Like Au, Pt, Pd, Ag, or Cu Electrode Catalysts in Nonthermal Atmospheric-Pressure Plasma of N_2 and H_2. *ACS Catal.* **2017**, *7*, 6924−6929.
(12) Groysman, S.; Holm, R. H. Biomimetic Chemistry of Iron, Nickel, Molybdenum, and Tungsten in Sulfur-Ligated Protein Sites†. *Biochemistry* **2009**, *48*, 2310−2320.
(13) Yao, Y.; Zhu, S.; Wang, H.; Li, H.; Shao, M. A Spectroscopic Study on the Nitrogen Electrochemical Reduction Reaction on Gold and Platinum Surfaces. *J. Am. Chem. Soc.* **2018**, *140*, 1496−1501.
(14) Medford, A. J.; Hatzell, M. C. Photon-Driven Nitrogen Fixation: Current Progress, Thermodynamic Considerations, and Future Outlook. *ACS Catal.* **2017**, *7*, 2624−2643.
(15) Comer, B. M.; Liu, Y. H.; Dixit, M. B.; Hatzell, K. B.; Ye, Y.; Crumlin, E. J.; Hatzell, M. C.; Medford, A. J. The Role of Adventitious Carbon in Photo-catalytic Nitrogen Fixation by Titania. *J. Am. Chem. Soc.* **2018**, *140*, 15157−15160.
(16) Edel, K.; Krieg, M.; Grote, D.; Bettinger, H. F. Photoreactions of Phenylborylene with Dinitrogen and Carbon Monoxide. *J. Am. Chem. Soc.* **2017**, *139*, 15151−15159.
(17) Minteer, S. D.; Christopher, P.; Linic, S. Recent Developments in Nitrogen Reduction Catalysts: A Virtual Issue. *ACS Energy Lett.* **2019**, *4*, 163−166.
(18) Liu, H.; Wei, L.; Liu, F.; Pei, Z.; Shi, J.; Wang, Z.-j.; He, D.; Chen, Y. Homogeneous, Heterogeneous, and Biological Catalysts for Electrochemical N_2 Reduction toward NH_3 under Ambient Conditions. *ACS Catal.* **2019**, *9*, 5245−5267.
(19) Geri, J. B.; Shanahan, J. P.; Szymczak, N. K. Testing the Push-Pull Hypothesis: Lewis Acid Augmented N_2 Activation at Iron. *J. Am. Chem. Soc.* **2017**, *139*, 5952−5956.
(20) Musaev, D. G. Theoretical prediction of a new dinitrogen reduction process: Utilization of four dihydrogen molecules and a Zr_2Pt_2 cluster. *J. Phys. Chem. B* **2004**, *108*, 10012−10018.
(21) Legare, M. A.; Belanger-Chabot, G.; Dewhurst, R. D.; Welz, E.; Krummenacher, I.; Engels, B.; Braunschweig, H. Nitrogen fixation and reduction at boron. *Science* **2018**, *359*, 896−900.
(22) Ling, C.; Niu, X.; Li, Q.; Du, A.; Wang, J. Metal-Free Single Atom Catalyst for N_2 Fixation Driven by Visible Light. *J. Am. Chem. Soc.* **2018**, *140*, 14161−14168.
(23) Bauschlicher, C. W.; Pettersson, L. G. M.; Siegbahn, P. E. M. The bonding in FeN_2, FeCO, and Fe_2N_2: Model systems for side-on bonding of CO and N_2. *J. Chem. Phys.* **1987**, *87*, 2129−2137.
(24) Yandulov, D. V.; Schrock, R. R. Catalytic reduction of dinitrogen to ammonia at a single molybdenum center. *Science* **2003**, *301*, 76−78.
(25) Arashiba, K.; Miyake, Y.; Nishibayashi, Y. A molybdenum complex bearing PNP-type pincer ligands leads to the catalytic reduction of dinitrogen into ammonia. *Nat. Chem.* **2011**, *3*, 120.
(26) Chalkley, M. J.; Del Castillo, T. J.; Matson, B. D.; Peters, J. C. Fe-Mediated Nitrogen Fixation with a Metallocene Mediator: Exploring pK_a Effects and Demonstrating Electrocatalysis. *J. Am. Chem. Soc.* **2018**, *140*, 6122−6129.
(27) Lindley, B. M.; Appel, A. M.; Krogh-Jespersen, K.; Mayer, J. M.; Miller, A. J. M. Evaluating the Thermodynamics of Electrocatalytic N_2 Reduction in Acetonitrile. *ACS Energy Lett.* **2016**, *1*, 698−704.
(28) Fryzuk, M. D. Side-on End-on Bound Dinitrogen: An Activated Bonding Mode That Facilitates Functionalizing Molecular Nitrogen. *Acc. Chem. Res.* **2009**, *42*, 127−133.
(29) Anderson, J. S.; Rittle, J.; Peters, J. C. Catalytic conversion of nitrogen to ammonia by an iron model complex. *Nature* **2013**, *501*, 84−87.
(30) Thompson, N. B.; Green, M. T.; Peters, J. C. Nitrogen Fixation via a Terminal Fe(IV) Nitride. *J. Am. Chem. Soc.* **2017**, *139*, 15312−15315.
(31) Lu, E.; Atkinson, B. E.; Wooles, A. J.; Boronski, J. T.; Doyle, L. R.; Tuna, F.; Cryer, J. D.; Cobb, P. J.; Vitorica-Yrezabal, I. J.; Whitehead, G. F. S.; Kaltsoyannis, N.; Liddle, S. T. Back-bonding between an electron-poor, high-oxidation-state metal and poor pi-acceptor ligand in a uranium(V)-dinitrogen complex. *Nat. Chem.* **2019**, *11*, 806−811.
(32) Power, P. P. Main-group elements as transition metals. *Nature* **2010**, *463*, 171−177.
(33) Kurzbach, D.; Sharma, A.; Sebastiani, D.; Klinkhammer, K. W.; Hinderberger, D. Dinitrogen complexation with main group radicals. *Chem. Sci.* **2011**, *2*, 473−479.
(34) Zheng, S.; Li, S.; Mei, Z.; Hu, Z.; Chu, M.; Liu, J.; Chen, X.; Pan, F. Electrochemical Nitrogen Reduction Reaction Performance of Single-Boron Catalysts Tuned by MXene Substrates. *J. Phys. Chem. Lett.* **2019**, *10*, 6984−6989.
(35) Liu, C.; Li, Q.; Wu, C.; Zhang, J.; Jin, Y.; MacFarlane, D. R.; Sun, C. Single-Boron Catalysts for Nitrogen Reduction Reaction. *J. Am. Chem. Soc.* **2019**, *141*, 2884−2888.
(36) Qiu, W.; Xie, X. Y.; Qiu, J.; Fang, W. H.; Liang, R.; Ren, X.; Ji, X.; Cui, G.; Asiri, A. M.; Cui, G.; Tang, B.; Sun, X. High-performance artificial nitrogen fixation at ambient conditions using a metal-free electrocatalyst. *Nat. Commun.* **2018**, *9*, 3485.
(37) Ji, S.; Wang, Z.; Zhao, J. A boron-interstitial doped C_2N layer as a metal-free electrocatalyst for N_2 fixation: a computational study. *J. Mater. Chem. A* **2019**, *7*, 2392−2399.
(38) Bhattacharyya, K.; Datta, A. Visible light driven efficient metal free single atom catalyst supported on nanoporous carbon nitride for nitrogen fixation. *Phys. Chem. Chem. Phys.* **2019**, *21*, 12346−12352.
(39) Zhang, J.; Zhao, Y.; Wang, Z.; Yang, G.; Tian, J.; Ma, D.; Wang, Y. Boron-decorated C_9N_4 monolayers as promising metal-free catalysts for electrocatalytic nitrogen reduction reaction: a first-principles study. *New J. Chem.* **2020**, *44*, 422−427.
(40) Mao, X.; Zhou, S.; Yan, C.; Zhu, Z.; Du, A. A single boron atom doped boron nitride edge as a metal-free catalyst for N_2 fixation. *Phys. Chem. Chem. Phys.* **2019**, *21*, 1110−1116.
(41) Chen, C.; Yan, D.; Wang, Y.; Zhou, Y.; Zou, Y.; Li, Y.; Wang, S. BN Pairs Enriched Defective Carbon Nanosheets for Ammonia Synthesis with High Efficiency. *Small* **2019**, *15*, No. e1805029.
(42) Li, Q. S.; Xu, Y. A quantum chemistry study: a new kind of boron nitrides. *J. Comput. Chem.* **2007**, *28*, 1446−1455.
(43) Khaliullin, R. Z.; Cobar, E. A.; Lochan, R. C.; Bell, A. T.; Head-Gordon, M. Unravelling the origin of intermolecular interactions using absolutely localized molecular orbitals. *J. Phys. Chem. A* **2007**, *111*, 8753−8765.
(44) Alkorta, I.; Elguero, J.; Del Bene, J. E.; Mo, O.; Yanez, M. New insights into factors influencing B-N bonding in X:BH(3-n)F(n) and X:BH(3-n)Cl(n) for X = N_2, HCN, LiCN, H_2CNH, NF_3, NH_3 and n = 0−3: the importance of deformation. *Chem. - Eur. J.* **2010**, *16*, 11897−905.
(45) Smith, E. L.; Sadowsky, D.; Phillips, J. A.; Cramer, C. J.; Giesen, D. J. A short yet very weak dative bond: structure, bonding, and energetic properties of N_2-BH_3. *J. Phys. Chem. A* **2010**, *114*, 2628−2636.
(46) Meisner, J.; Zhu, X.; Martinez, T. J. Computational Discovery of the Origins of Life. *ACS Cent. Sci.* **2019**, *5*, 1493−1495.

https://dx.doi.org/10.1021/jacs.0c00409
J. Am. Chem. Soc. 2020, 142, 6244−6250

(47) De Angelis, P.; Cardellini, A.; Asinari, P. Exploring the Free Energy Landscape To Predict the Surfactant Adsorption Isotherm at the Nanoparticle-Water Interface. *ACS Cent. Sci.* **2019**, *5*, 1804−1812.
(48) Chai, J.-D.; Head-Gordon, M. Long-range corrected hybrid density functionals with damped atom-atom dispersion corrections. *Phys. Chem. Chem. Phys.* **2008**, *10*, 6615−6620.
(49) Frisch, M. J.; Trucks, G. W.; Schlegel, H. B.; Scuseria, G. E.; Robb, M. A.; Cheeseman, J. R.; Scalmani, G.; Barone, V.; Mennucci, B.; Petersson, G. A.; Nakatsuji, H.; Caricato, M.; Li, X.; Hratchian, H. P.; Izmaylov, A. F.; Bloino, J.; Zheng, G.; Sonnenberg, J. L.; Hada, M.; Ehara, M.; Toyota, K.; Fukuda, R.; Hasegawa, J.; Ishida, M.; Nakajima, T.; Honda, Y.; Kitao, O.; Nakai, H.; Vreven, T.; Montgomery, J. A., Jr.; Peralta, J. E.; Ogliaro, F.; Bearpark, M.; Heyd, J. J.; Brothers, E.; Kudin, K. N.; Staroverov, V. N.; Kobayashi, R.; Normand, J.; Raghavachari, K.; Rendell, A.; Burant, J. C.; Iyengar, S. S.; Tomasi, J.; Cossi, M.; Rega, N.; Millam, J. M.; Klene, M.; Knox, J. E.; Cross, J. B.; Bakken, V.; Adamo, C.; Jaramillo, J.; Gomperts, R.; Stratmann, R. E.; Yazyev, O.; Austin, A. J.; Cammi, R.; Pomelli, C.; Ochterski, J. W.; Martin, R. L.; Morokuma, K.; Zakrzewski, V. G.; Voth, G. A.; Salvador, P.; Dannenberg, J. J.; Dapprich, S.; Daniels, A. D.; Farkas, O.; Foresman, J. B.; Ortiz, J. V.; Cioslowski, J.; Fox, D. J. *Gaussian 09*, revision B.01; Gaussian, Inc.: Wallingford, CT, 2009.
(50) Marenich, A. V.; Cramer, C. J.; Truhlar, D. G. Universal solvation model based on solute electron density and on a continuum model of the solvent defined by the bulk dielectric constant and atomic surface tensions. *J. Phys. Chem. B* **2009**, *113*, 6378−6396.
(51) Tomasi, J.; Persico, M. Molecular-Interactions in Solution - an Overview of Methods Based on Continuous Distributions of the Solvent. *Chem. Rev.* **1994**, *94*, 2027−2094.
(52) Hermans, J.; Wang, L. Inclusion of Loss of Translational and Rotational Freedom in Theoretical Estimates of Free Energies of Binding. Application to a Complex of Benzene and Mutant T4 Lysozyme. *J. Am. Chem. Soc.* **1997**, *119*, 2707−2714.
(53) Ma, X.; Lei, M. Mechanistic Insights into the Directed Hydrogenation of Hydroxylated Alkene Catalyzed by Bis(phosphine) cobalt Dialkyl Complexes. *J. Org. Chem.* **2017**, *82*, 2703−2712.
(54) Li, L.; Zhu, H.; Liu, L.; Song, D.; Lei, M. A Hydride-Shuttle Mechanism for the Catalytic Hydroboration of CO_2. *Inorg. Chem.* **2018**, *57*, 3054−3060.
(55) Mammen, M.; Shakhnovich, E. I.; Deutch, J. M.; Whitesides, G. M. Estimating the Entropic Cost of Self-Assembly of Multiparticle Hydrogen-Bonded Aggregates Based on the Cyanuric Acid÷Melamine Lattice. *J. Org. Chem.* **1998**, *63*, 3821−3830.
(56) Glendening, E. D.; Badenhoop, J. K.; Reed, A. E.; Carpenter, J. E.; Bohmann, J. A.; Morales, C. M.; Landis, C. R.; Weinhold, F. NBO 6.0: Natural Bond Orbital Analysis Programs. *J. Comput. Chem.* **2013**, *34*, 2134.
(57) Oshima, K.; Ohmura, T.; Suginome, M. Dearomatizing conversion of pyrazines to 1,4-dihydropyrazine derivatives via transition-metal-free diboration, silaboration, and hydroboration. *Chem. Commun.* **2012**, *48*, 8571−8753.
(58) Ohmura, T.; Morimasa, Y.; Suginome, M. Organocatalytic diboration involving "reductive addition" of a boron-boron sigma-bond to 4,4′-bipyridine. *J. Am. Chem. Soc.* **2015**, *137*, 2852−2855.
(59) Neeve, E. C.; Geier, S. J.; Mkhalid, I. A.; Westcott, S. A.; Marder, T. B. Diboron(4) Compounds: From Structural Curiosity to Synthetic Workhorse. *Chem. Rev.* **2016**, *116*, 9091−9161.
(60) Borden, W. T. Why Are Addition Reactions to N_2 Thermodynamically Unfavorable? *J. Phys. Chem. A* **2017**, *121*, 1140−1144.

https://dx.doi.org/10.1021/jacs.0c00409
J. Am. Chem. Soc. 2020, 142, 6244−6250